**Indonesian Journal of Electrical Engineering and Computer Science**
Vol. 35, No. 3, September 2024, pp. 1670~1679
ISSN: 2502-4752, DOI: 10.11591/ijeecs.v35.i3.pp1670-1679 

# Biomedical image classification using seagull optimization with deep learning for colon and lung cancer diagnosis

**Thiyagarajan Manoharan[1], Ramalingam Velvizhi[2], Tarun Kumar Juluru[3], Shoaib Kamal[4], Shrabani Mallick[5], Ezudheen Puliyanjalil[6]**
[1]Computer Science and Engineering, Vel Tech Rangarajan Dr. Sagunthala R&D Institute of Science and Technology, Chennai, India
[2]Department of Computer Science and Engineering, Sathyabama Institute of Science and Technology, (Deemed to be University), Chennai, India
[3]Department of Electrical and Computer Engineering, Kakatiya Institute of Technology and Science, Warangal, India
[4]Department of Electrical and Computer Engineering, Dr. B. R. Ambedkar Institute of Technology, Port Blair, India
[5]Department of Computer Science and Engineering, Dr. B. R. Ambedkar Institute of Technology, Port Blair, India
[6]Computer Science and Engineering, Government Engineering College Thrissur, Thrissur Engineering College P O, Thrissur, India

**Article Info**

***Article history:***

Received Feb 11, 2024
Revised Apr 20, 2024
Accepted May 7, 2024

***Keywords:***

Deep learning
Magnetic resonance imaging
Medical imaging
Seagull optimization algorithm
X-ray

**ABSTRACT**

Traditional health care relies on biomedical image categorization to identify and treat various medical conditions. In machine learning and medical imaging, biomedical image classification for colon and lung cancer diagnosis is significant. The work focuses on building novel models and algorithms to accurately detect and categorize tumorous lesions using computer tomography (CT) scans and histopathology slides. These systems use image processing, deep learning (DL), and convolutional neural networks (CNN) to assist medical professionals diagnose cancer sooner and improve patient outcomes. Biomedical image classification using seagull optimization with deep learning (BIC-SGODL) addresses colon and lung cancer diagnosis. The BIC-SGODL method improves cancer diagnosis using hyperparameter optimized DL model. BIC-SGODL utilizes DenseNet to learn complicated features. The convolutional long short-term memory (CLSTM) standard captures spatiotemporal information in sequential picture data. Finally, the SGO method adjusts hyperparameters to improve model performance and generalization. BIC-SGODL performs well with biomedical image dataset simulations. Thus, medical picture cancer diagnosis may be automated using BIC-SGODL.



***Corresponding Author:***

Ezudheen Puliyanjalil
Computer Science and Engineering, Government Engineering College Thrissur
Thrissur Engineering College P O
Thrissur, Kerala-680009, India
Email: ezudheenpuliyanjalil@gmail.com

## 1. INTRODUCTION

Medical imaging is essential for non-invasive analytic procedures in modern healthcare [1]. Visualization and depiction of the human body and organs for clinical study are included. Computerized tomography (CT), mammography, conventional X-ray, ultrasound (US), magnetic resonance imaging (MRI), and molecular imaging are all available [2]. Clinical pictures are used to detect many skin-related conditions, notwithstanding medical imaging models [3]. Medical imaging has two parts: image production and reconstruction and image processing and analysis. The image generation approach creates 2D pictures of 3D objects while developing confidence in iterative models to spontaneously produce 2D and 3D imageries from object prediction data [4]. Picture processing uses techniques to improve picture qualities including noise

extraction, whereas image analysis eliminates assessable data or attributes for object identification or detection [5].

Compared to machine learning (ML), deep learning (DL) models are often used to get better, scalable, and accurate data results [6]. DL is also utilized in biomedical imaging to diagnose disorders and provide individualized therapy to improve patient health. Electrocardiogram (ECG), electroencephalography (EEG), MRI, magnetoencephalography (MEG), and others are common biomedical imaging methods for patient diagnosis that minimize human participation [7]. Medical photos include noise, making analysis difficult. A branch of AI ML is DL. It focuses on brain-inspired approaches [8]. Computing approaches may test dataset representation with several hidden processing layers [9].

They worry about feature extraction and transformation. Next layer receives last layer output. The best way to automate analytical study [10]. Both supervised and unsupervised methods provide great results. Our seagull optimization with deep learning (BIC-SGODL) biomedical image classification method diagnoses colon and lung cancer. The BIC-SGODL method improves cancer diagnosis using hyperparameter optimized DL model. BIC-SGODL utilizes DenseNet to learn complicated features. Convolutional long short-term memory (CLSTM) captures spatiotemporal information in sequential picture data. Finally, the SGO method adjusts hyperparameters to improve model performance and generalization. BIC-SGODL performs well with biomedical imaging dataset simulation analysis.

## 2. RELATED WORKS

An effective and precise lung cancer (LC) classification method was developed in [11]. This study improved EfficientNetB0 and ResNet50 DL algorithms. Normal distribution-based grey wolf optimizer (GWO) was used to gain superior features for 5 classifiers. Soft voting uses these 5 models' results. Semi-supervised methods are described in [12]. Hypergraph neural networks are used for categorization in this paper. Initial picture deep feature removal at input patches was done by pre-trained VGG19. A hypergraph was constructed using patch-level deep features to represent hyperedge vertices and pair-wise Euclidean distance to allocate it. Ragab *et al.* [13] developed DHODCNNLCC, a deer hunting optimizer with deep-convolutional neural network (deep-CNN) for lung cancer detection and classification. Features are extracted from preprocessed pictures using the Nadam optimizer with RefineDet architecture.

In addition, lung lesions were classified using denoising stacked-AE (DSAE). Finally, the optimal hyperparameters were tuned using the deer hunting optimizer algorithm (DHOA). Ullah *et al.* [14] developed DeepLCCNet to classify five LC tissues (two benign and three malignant). The approach classified five tissue types of LC cancer HI database: lung, colon, squamous cell lung cancer, benign colon tissue, and benign lung tissue. A multi-classification DL method for lung cancer, COVID-19, and pneumonia using CT and chest X-ray (CXR) images was established in [15]. Four frameworks-ResNet152V2+GRU, ResNet152V2, VGG19-CNN, and bidirectional gated recurrent unit (BiGRU)-are also evaluated.

Mohalder *et al.* [16] proposed DL colorectal cancer (CRC) diagnosis. CNN was used to identify complex data. CNN has been used to identify suspicious or aberrant malignant patterns in challenging cancerous pictures. A 5-layer deep neural network (DNN) may result. It has 4 hidden, input, and output layers. Softmax may be used in the output layer and rectified linear unit (ReLU) in the hidden layers. Kadirappa *et al.* [17], DL-based cancer detection was described. CNNs eliminate features in DL models. DeepHistoNet, a densely linked residual, attention-guided, and dilated convolution-DNN, produces reliable classification patterns.

## 3. THE PROPOSED MODEL

This article paper an introduces BIC-SGODL method for Colon and lung cancer diagnosis. The presented BIC-SGODL technique exploits hyperparameter tuned DL model for improved cancer detection results. Figure 1 demonstrates the entire procedure of BIC-SGODL algorithm.

### 3.1. DenseNet model

It signifies an innovative architectural novelty in the domain of DL for the image classification task. DenseNet presents densely connected layers or blocks in the network structure unlike classical CNN. All the layers are interconnected to all the succeeding layers, enabling gradient propagation and direct information flow. This unique connectivity pattern inspires feature reuse, alleviates the vanishing gradient problem, and leads to parameter-efficient and highly efficient models. The remarkable performance of DenseNet has made it a foundation stone in CV applications, encompassing image classification, object detection, and segmentation, constantly accomplishing advanced outcomes with less parameters, allowing interpretable and more robust DL outcomes. In postmortem studies, primary lung cancer spreads to the gastrointestinal tract more often than previously thought [18]. Artificial intelligent (AI) can automate cancer diagnosis, allowing

us to examine more patients faster and cheaper. This study uses modern DL and digital image processing (DIP) methods to classify five lung and colon tissues [19], [20].

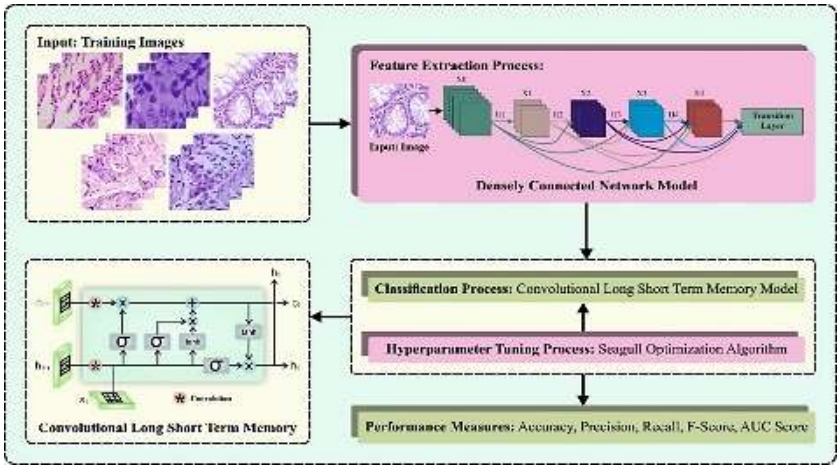


Figure 1. Overall process of BIC-SGODL system

### 3.2. CLSTM based classification

The memory units, forget, input, and output gates are the building blocks of LSTM [21]. The formula for input, forget, and output gates, together with the cell status, the output of LSTM cells, and the candidate cell status, are correspondingly shown as (1) to (6):

$$i_t = \sigma(W_{hi}h_{t-1} + W_{xi}x_t + b_i) \quad (1)$$

$$f_t = \sigma(W_hfh_{t-1} + W_xfx_t + bf) \quad (2)$$

$$0_t = \sigma(W_{ho}h_{t-1} + W_{xo}x_t + b_0) \quad (3)$$

$$C_t = tanh(W_{hC}h_{t-1} + W_{xC}x_t + b_C) \quad (4)$$

$$C_t = f_tC_{t-1} + (1 - f_t)\tilde{C}_t \quad (5)$$

$$h_t = 0_ttanh(C_t) \quad (6)$$

Here, the forget gate refers to $f$, the input gate represents $i$, the candidate cell state shows $C_t$, the output gate indicates 0, the hidden state and cell output denotes $h$, the cell state represents $C$, the weight matrix shows $W$, the bias vector denotes $b$, and a logistic sigmoid function signifies $\sigma$.

ConvLSTM is a special type of LSTM that is intended to accurately design the spatial-temporal information, by leveraging the capability of LSTM and CNN. Similar to LSTM, the ConvLSTM can able to decide which information must be retained or discarded from the past cell status. In contrast, convolutional model is exploited on input-to-state and state-to-state conversions that generally interchange matrix multiplication with convolution function. The input vector to ConvLSTM is provided as a series of 2D or 3D images meanwhile the convolution function allows the data that passed through ConvLSTM cells to retain the inputted dimension instead of 1D with feature vector. To describe the ConvLSTM function the given expression is as (7) to (12).

$$i_t = \sigma(W_{Ci} \circ C_{t-1} + W_{hi} * h_{t-1} + W_{xi} * x_t + b_i) \quad (7)$$

$$f_t = \sigma\left(W_Cf \circ C_{t-1} + W_{hf} * h_{t-1} + W_{xf} * x_t + b_f\right) \quad (8)$$

$$0_t = \sigma(W_{Co} \circ C_t + W_{ho} * h_{t-1} + W_{xo} * x_t + b_0) \quad (9)$$

$$C_t = tanh(W_{hC} * h_{t-1} + W_{xC} * x_t + b_C) \quad (10)$$

$$C_t = f_t \circ C_{t-1} + (1 - f_t) \circ \tilde{C}_t \quad (11)$$

$$h_t = 0_t \circ tanh(C_t) \quad (12)$$

Where the Hadamard product $\circ$, the convolution operators show $*$, the convolutional kernels are $W_{Ci}$, $W_{hi}$, $W_{xi}, W_C, W_h, W_x, W_{Co}, W_{ho}, W_{xo}, W_{hC}, W_{xC} \in \mathbb{R}^{n \times T}$, and the bias parameter is $b_i$, $b_f$, $b_0, b_C$. The ConvLSTM model, where the red line specifies the further connection was established in ConvLSTM over LSTM cells that derive from existing and preceding cell status.

### 3.3. SGO based hyperparameter tuning

SGO technique is derived from the migrating and attacking strategies of seagulls. During the migration, the method simulates how seagulls move all over the place [22]. The variable $A$ is added for computing the newest position of search agent to prevent conflict among them.

$$\vec{C}_s = A \times \vec{P}_s(x) \quad (13)$$

Where the location of search agent which doesn't conflict with others is $\vec{C}_s$, existing location of the search agent signifies $\vec{P}_s$, existing iteration time is $x$, and the mobile behaviors of search agent in a search range is $A$.

$$A = f_c - \left( x \times \left( \frac{f_c}{\text{Max}_{\text{iteration}}} \right) \right) \quad (14)$$

Where $x = 0, 1, 2, \ldots, \text{Max}_{\text{iteration}}$, while $f_c$ controls the usage frequency of variable $A$, that is linearly reduced from *fc* to 0, and in this study $f_c$ is fixed to two. When avoiding collisions among seagulls, the search agent moves in the direction of optimum neighbor.

$$\vec{M}_s = B \times \left( \vec{P}_{bs}(x) - \vec{P}_s(x) \right) \quad (15)$$

Where the optimal search agent is $\vec{P}_s$, location of search agent is $\vec{M}_s$, fittest seagull using lesser fitness value is $P_{bs}$. The behavior of $B$ is random which balances among exploitation and exploration.

$$B = 2 \times A^2 \times \text{rd} \quad (16)$$

Here arbitrary number ranges within [0,1] is $rd$. Finally, the search agent upgrades the location. Figure 2 depicts the flowchart of SGO method.

$$\vec{D}_s = \left| \vec{C}_s + \vec{M}_s \right| \quad (17)$$

Where $\vec{D}_s$ denotes distance among the search agent and optimum search agent (viz., optimal seagulls where the fitness value is smaller). In the procedure of attacking prey, seagulls would spiral movement in the air given by:

$$x' = r \times \cos(k) \quad (18)$$

$$y' = r \times \sin(k) \quad (19)$$

$$z' = r \times k \quad (20)$$

$$r = u \times e^{kv} \quad (21)$$

Whereas $r$ denotes radius of every spiral turn and arbitrary amount in the range $[0, 2\pi]$ shows $k$. The base of natural logarithm is $e$, and constants $u$ and $v$ define the spiral formation is shown in (22).

$$\vec{P}_s(x) = \left( \vec{D}_s \times x' \times y' \times z' \right) + \vec{P}_{bs}(x) \quad (22)$$

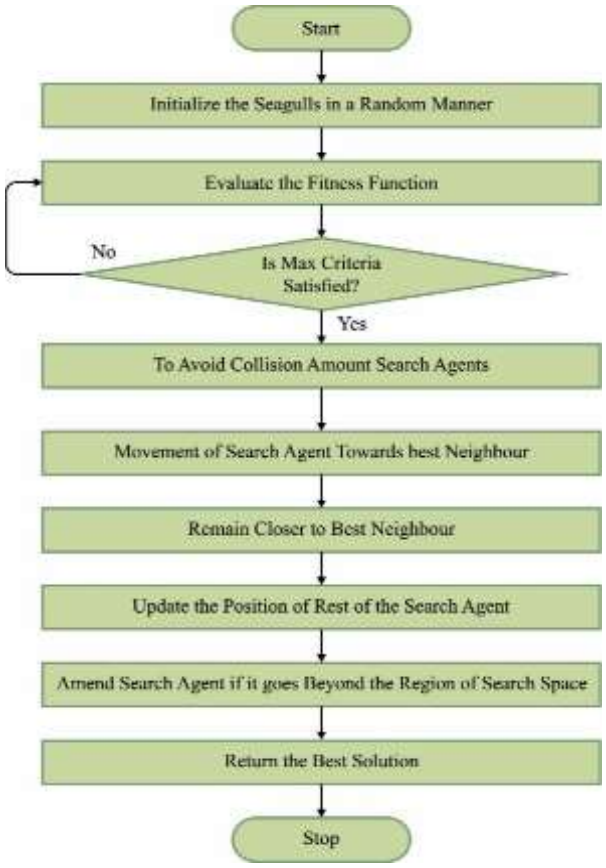


Figure 2. Flowchart of SGO

## 4. RESULT ANALYSIS AND DISCUSSION

The classification outcomes of the BIC-SGODL method is examined on the medical dataset [23] including 25,000 instances and five classes as described in Table 1.

Table 1. Facts on dataset

| Class name | Description | No. of instances |
|---|---|---|
| Col_Ad | Colon adenocarcinoma | 5,000 |
| Col_Be | Colon benign tissue | 5,000 |
| Lun_Ad | Lung adenocarcinoma | 5,000 |
| Lun_Be | Lung benign tissue | 5,000 |
| Lun_SC | Lung squamous cell carcinoma | 5,000 |
| | Total no. of instances | 25,000 |

Figure 3 illustrates the classifier analysis of the BIC-SGODL method under test dataset. Figures 3(a) to 3(b) shows the confusion matrices given by the BIC-SGODL model on 70:30 of TR phase/TS phase. The outcome indicated that the BIC-SGODL model has appropriately recognized and categorized 5 classes. Additionally, Figure 3(c) exhibits the PR investigation of the BIC-SGODL method. The simulation value shown that the BIC-SGODL model is gained higher PR performance with every classes. Besides, Figure 3(d) represents the ROC analysis of the BIC-SGODL model. This outcome revealed that the BIC-SGODL system leads to proficient outcomes with greater ROC values with various classes.

In Table 2 and Figure 4, the detection outcomes of the BIC-SGODL technique is clearly demonstrated. The simulated outcome shows that the BIC-SGODL method gets enhanced outcomes with every class. With 70% of TR Phase, the BIC-SGODL system provides average $accu_y$, $prec_n$, $reca_l$, $F_{score}$, and $AUC_{score}$ of 99.43%, 98.59%, 98.58%, 98.58%, and 99.11% respectively. Also, on 30% of TS Phase, the BIC-SGODL methodology gives average $accu_y$, $prec_n$, $reca_l$, $F_{score}$, and $AUC_{score}$ of 99.45%, 98.62%, 98.61%, 98.62%, and 99.13% correspondingly.

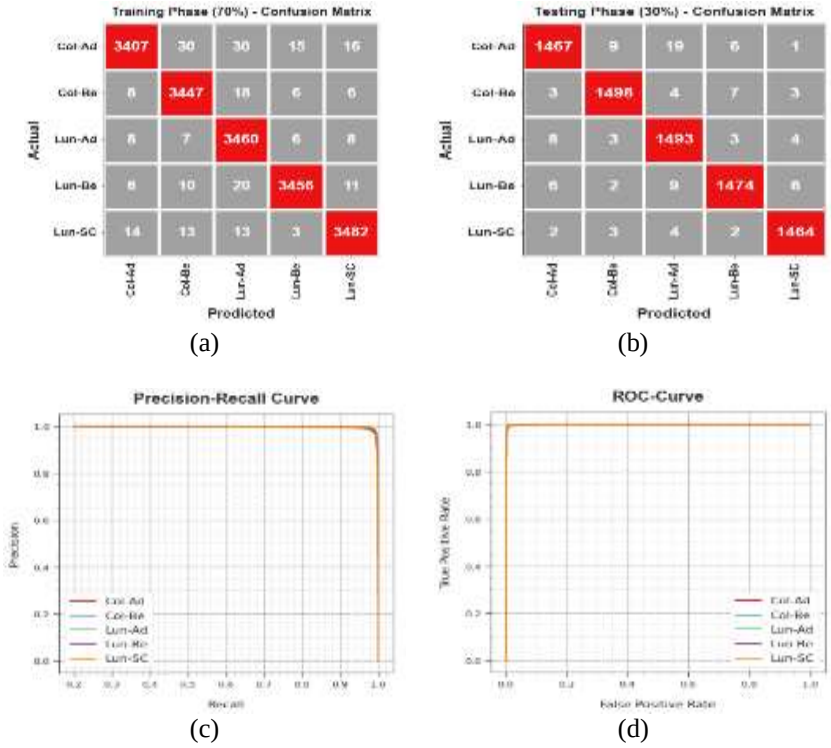


Figure 3. Classifier outcome of: (a) confusion matrices, (b) confusion matrices, (c) PR curve, and (d) ROC curve

Table 2. Detection outcome of BIC-SGODL system on 70:30 of TR phase/TS phase

| | Classes | $Accu_y$ | $Prec_n$ | $Reca_l$ | $F_{score}$ | $AUC_{score}$ |
|---|---|---|---|---|---|---|
| TR phase (70%) | Col_Ad | 99.27 | 98.95 | 97.40 | 98.17 | 98.57 |
| | Col_Be | 99.44 | 98.29 | 98.91 | 98.60 | 99.24 |
| | Lun_Ad | 99.37 | 97.71 | 99.17 | 98.44 | 99.30 |
| | Lun_Be | 99.56 | 99.14 | 98.66 | 98.90 | 99.22 |
| | Lun_SC | 99.52 | 98.84 | 98.78 | 98.81 | 99.24 |
| | **Average** | **99.43** | **98.59** | **98.58** | **98.58** | **99.11** |
| TS phase (30%) | Col_Ad | 99.28 | 98.72 | 97.67 | 98.19 | 98.68 |
| | Col_Be | 99.55 | 98.88 | 98.88 | 98.88 | 99.30 |
| | Lun_Ad | 99.28 | 97.65 | 98.81 | 98.22 | 99.10 |
| | Lun_Be | 99.45 | 98.79 | 98.46 | 98.63 | 99.08 |
| | Lun_SC | 99.67 | 99.05 | 99.25 | 99.15 | 99.51 |
| | **Average** | **99.45** | **98.62** | **98.61** | **98.62** | **99.13** |

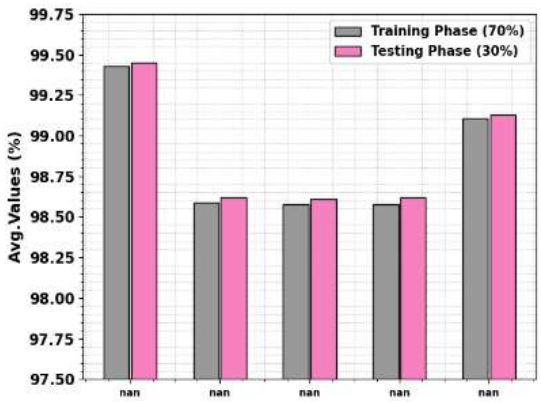


Figure 4. Average of BIC-SGODL method at 70:30 of TR phase/TS phase

Figure 5 shows accuracy curves for the training (TR) and testing (TS) phases of the BIC-SGODL approach to assess its efficacy. These graphs show the model's generalization capacity and learning growth. As epochs increase, TR and TS accu_y curves improve. The model can better detect trends in the TR and TS datasets. Table 3 provides a full BIC-SGODL technique comparison. The BIC-SGODL technique improves results [24], [25]. Figure 6 compares BIC-SGODL's accu_y performance. BIC-SGODL has accu_y of 99.45%, whereas MPADLLC3, m-SRC, fast region-based convolutional neural network (RCNN), DAEL-GNN, ResNet50, CN, and DL have accu_y of 98.81%, 88.25%, 98.70%, 98.56%, 93.96%, 97.05%, and 96.29%.

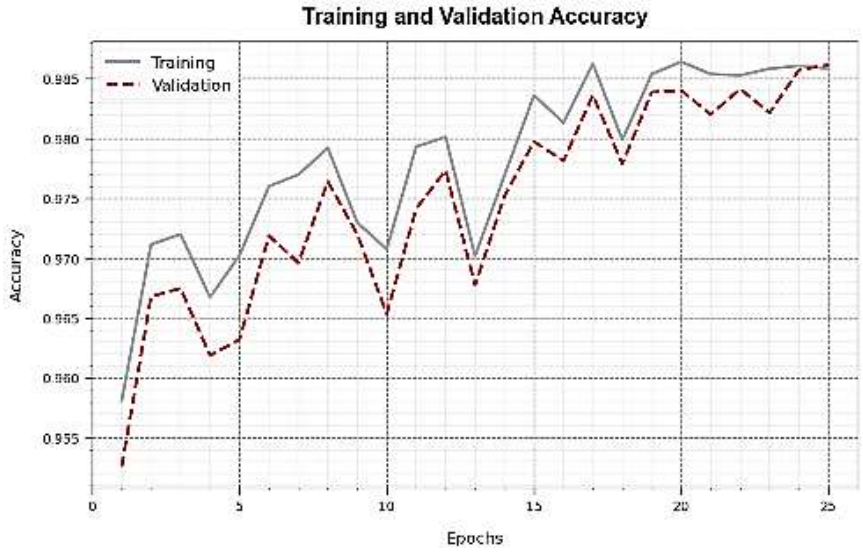


Figure 5. $Accu_y$ curve of BIC-SGODL model with TR and TS phase

Table 3. Comparative result of BIC-SGODL algorithm with existing methods

| Methods | $Accu_y$ | $Prec_n$ | $Reca_l$ | $F_{score}$ |
|---|---|---|---|---|
| BIC-SGODL | 99.45 | 98.62 | 98.61 | 98.62 |
| MPADLLC3 | 98.81 | 97.92 | 97.87 | 97.91 |
| m-SRC | 88.25 | 85.20 | 91.74 | 86.66 |
| Fast RCNN | 98.70 | 96.44 | 97.84 | 97.28 |
| DAEL-GNN | 98.56 | 98.08 | 96.56 | 96.65 |
| RESNET50 | 93.96 | 96.28 | 97.48 | 96.95 |
| CNN | 97.05 | 96.92 | 97.41 | 97.74 |
| DL | 96.29 | 96.96 | 96.14 | 98.03 |

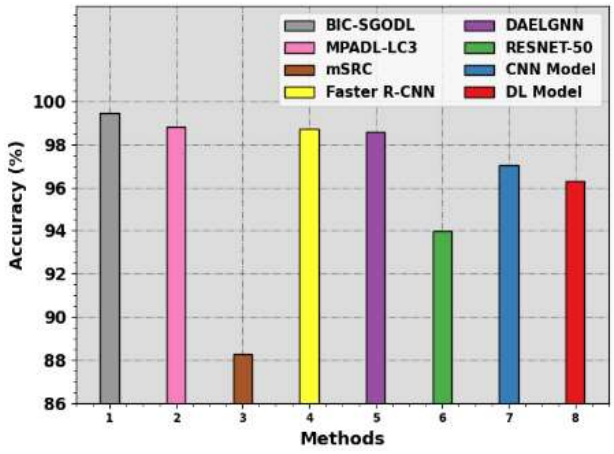


Figure 6. $Accu_y$ outcome of BIC-SGODL algorithm with recent approaches

Figure 7 exhibits the comparison performance of the BIC-SGODL technique with respect to $prec_n$, $reca_l$, $F_{score}$. According to $prec_n$, the BIC-SGODL system attains improved $prec_n$ of 98.62% whereas the MPADLLC3, m-SRC, faster RCNN, DAEL-GNN, ResNet50, CN, and DL methods get decreased $prec_n$ values of 97.92%, 85.20%, 96.44%, 98.08%, 96.28%, 96.92%, and 96.96%. Additionally, based on $reca_l$, the BIC-SGODL algorithm obtains better $reca_l$ of 98.61% but, MPADLLC3, m-SRC, Fast RCNN, DAEL-GNN, ResNet50, CN, and DL systems acquire reduced $reca_l$ values of 97.87%, 91.74%, 97.84%, 96.56%, 97.48%, 97.41%, and 96.14%. Besides, with $F_{score}$, the BIC-SGODL methodology get increased $F_{score}$ of 98.62% whereas, the MPADLLC3, m-SRC, fast RCNN, DAEL-GNN, ResNet50, CN, and DL systems acquire diminished $F_{score}$ values of 97.91%, 91.74%, 97.84%, 96.56%, 97.48%, 97.41%, and 96.14%. Therefore, the BIC-SGODL technique is found to be suitable for medical image classification.

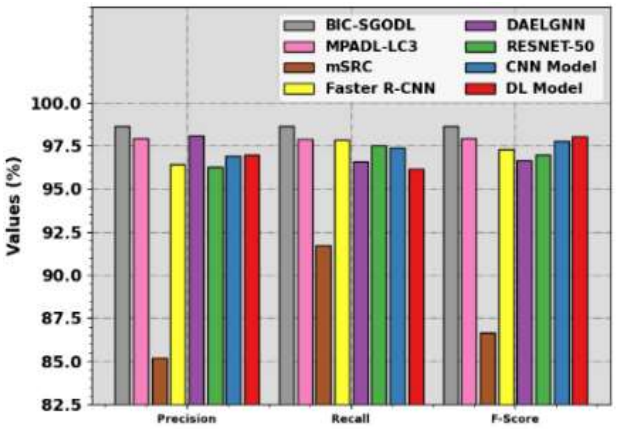


Figure 7. $Prec_n$, $reca_l$, and $F_{score}$ analysis of BIC-SGODL model with recent systems

## 5. CONCLUSION

This article introduces a BIC-SGODL technique for Colon and lung cancer diagnosis. The presented BIC-SGODL technique exploits hyperparameter tuned DL model for improved cancer detection results. To learn the intricate and complex features, the BIC-SGODL technique uses DenseNet model. The use of CLSTM helps to capture the spatiotemporal features, chiefly helpful for sequential image data. Finally, the SGO algorithm is employed for hyperparameter tuning, optimizing model performance and generalization. With comprehensive simulation analysis on biomedical image dataset, the BIC-SGODL technique illustrates considerable performance. Therefore, the BIC-SGODL technique can be employed for automated cancer detection on medical images.

## REFERENCES

[1] A. H. Chehade, N. Abdallah, J. M. Marion, M. Oueidat, and P. Chauvet, "Lung and colon cancer classification using medical imaging: a feature engineering approach," *Physical and Engineering Sciences in Medicine*, vol. 45, no. 3, pp. 729–746, 2022, doi: 10.1007/s13246-022-01139-x.

[2] M. Toğaçar, "Disease type detection in lung and colon cancer images using the complement approach of inefficient sets," *Computers in Biology and Medicine*, vol. 137, p. 104827, 2021, doi: 10.1016/j.compbiomed.2021.104827.

[3] I. Pacal, D. Karaboga, A. Basturk, B. Akay, and U. Nalbantoglu, "A comprehensive review of deep learning in colon cancer," *Computers in Biology and Medicine*, vol. 126, p. 104003, 2020, doi: 10.1016/j.compbiomed.2020.104003.

[4] O. Attallah, M. F. Aslan, and K. Sabanci, "A framework for lung and colon cancer diagnosis via lightweight deep learning models and transformation methods," *Diagnostics*, vol. 12, no. 12, p. 2926, 2022, doi: 10.3390/diagnostics12122926.

[5] M. A. Fahami, M. Roshanzamir, N. H. Izadi, V. Keyvani, and R. Alizadehsani, "Detection of effective genes in colon cancer: a machine learning approach," *Informatics in Medicine Unlocked*, vol. 24, p. 100605, 2021, doi: 10.1016/j.imu.2021.100605.

[6] M. S. S. N. Raju and B. S. Rao, "Lung and colon cancer classification using hybrid principle component analysis network-extreme learning machine," *Concurrency and Computation: Practice and Experience*, vol. 35, no. 1, 2023, doi: 10.1002/cpe.7361.

[7] M. A. Talukder, M. M. Islam, M. A. Uddin, A. Akhter, K. F. Hasan, and M. A. Moni, "Machine learning-based lung and colon cancer detection using deep feature extraction and ensemble learning," *Expert Systems with Applications*, vol. 205, p. 117695, 2022, doi: 10.1016/j.eswa.2022.117695.

[8] H. C. Reis and V. Turk, "Transfer learning approach and nucleus segmentation with MedCLNet colon cancer database," *Journal of Digital Imaging*, vol. 36, no. 1, pp. 306–325, 2023, doi: 10.1007/s10278-022-00701-z.

[9] N. Kumar, M. Sharma, V. P. Singh, C. Madan, and S. Mehandia, "An empirical study of handcrafted and dense feature extraction techniques for lung and colon cancer classification from histopathological images," *Biomedical Signal Processing and Control*, vol. 75, p. 103596, 2022, doi: 10.1016/j.bspc.2022.103596.

[10] M. Masud, N. Sikder, A. Al Nahid, A. K. Bairagi, and M. A. Alzain, "A machine learning approach to diagnosing lung and colon cancer using a deep learning-based classification framework," *Sensors (Switzerland)*, vol. 21, no. 3, p. 748, 2021, doi: 10.3390/s21030748.
[11] M. Ijaz *et al.*, "DS$^2$LC$^3$Net : a decision support system for lung colon cancer classification using fusion of deep neural networks and normal distribution based gray wolf optimization," *ACM Transactions on Asian and Low-Resource Language Information Processing*, 2023, doi: 10.1145/3625096.
[12] A. B. Bakht, S. Javed, H. Almarzouqi, A. Khandoker, and N. Werghi, "Colorectal cancer tissue classification using semi-supervised hypergraph convolutional network," in *Proceedings - International Symposium on Biomedical Imaging*, 2021, vol. 2021-April, pp. 1306–1309, doi: 10.1109/ISBI48211.2021.9434036.
[13] M. Ragab, H. A. Abdushkour, A. F. Nahhas, and W. H. Aljedaibi, "Deer hunting optimization with deep learning model for lung cancer classification," *Computers, Materials and Continua*, vol. 73, no. 1, pp. 533–546, 2022, doi: 10.32604/cmc.2022.028856.
[14] N. Ullah, I. De Falco, and G. Sannino, "A novel deep learning approach for colon and lung cancer classification using histopathological images," in *2023 IEEE 19th International Conference on e-Science (e-Science)*, 2023, pp. 1–10.
[15] D. M. Ibrahim, N. M. Elshennawy, and A. M. Sarhan, "Deep-chest: multi-classification deep learning model for diagnosing COVID-19, pneumonia, and lung cancer chest diseases," *Computers in Biology and Medicine*, vol. 132, p. 104348, 2021, doi: 10.1016/j.compbiomed.2021.104348.
[16] R. D. Mohalder, F. B. Ali, L. Paul, and K. H. Talukder, "Deep learning-based colon cancer tumor prediction using histopathological images," in *Proceedings of 2022 25th International Conference on Computer and Information Technology, ICCIT 2022*, 2022, pp. 629–634, doi: 10.1109/ICCIT57492.2022.10054766.
[17] R. Kadirappa, S. Deivalakshmi, R. Pandeeswari, and S. B. Ko, "DeepHistoNet: a robust deep-learning model for the classification of hepatocellular, lung, and colon carcinoma," *Microscopy Research and Technique*, vol. 87, no. 2, pp. 229–256, 2024, doi: 10.1002/jemt.24426.
[18] H. Sakai *et al.*, "Primary lung cancer presenting with metastasis to the colon: a case report," *World Journal of Surgical Oncology*, vol. 10, pp. 1–5, 2012, doi: 10.1186/1477-7819-10-127.
[19] S. Hadiyoso, S. Aulia, I. D. Irawati, "Diagnosis of lung and colon cancer based on clinical pathology images using convolutional neural network and CLAHE framework," *International Journal of Applied Science and Engineering*, vol. 20, no. 1, pp. 1-7, 2023.
[20] A. H. Chehade, N. Abdallah, J.-M. Marion, M. Oueidat, and P. Chauvet, "Lung and colon cancer classification using medical imaging: a feature engineering approach," *Physical and Engineering Sciences in Medicine* vol. 45, no. 3, pp. 729-746, doi: 10.1007/s13246-022-01139-x.
[21] W. Bao *et al.*, "An improved DenseNet model to classify the damage caused by cotton aphid," *Computers and Electronics in Agriculture*, vol. 203, p. 107485, 2022, doi: 10.1016/j.compag.2022.107485.
[22] B. Zhang, G. Zou, D. Qin, Q. Ni, H. Mao, and M. Li, "RCL-learning: ResNet and convolutional long short-term memory-based spatiotemporal air pollutant concentration prediction model," *Expert Systems with Applications*, vol. 207, p. 118017, 2022, doi: 10.1016/j.eswa.2022.118017.
[23] A. A. Ewees, R. R. Mostafa, R. M. Ghoniem, and M. A. Gaheen, "Improved seagull optimization algorithm using Lévy flight and mutation operator for feature selection," *Neural Computing and Applications*, vol. 34, no. 10, pp. 7437–7472, 2022, doi: 10.1007/s00521-021-06751-8.
[24] A. Maranhão, "Lung and colon cancer histopathological images," *Kaggle.com*, 2020. https://www.kaggle.com/datasets/andrewmvd/lung-and-colon-cancer-histopathological-images.
[25] M. Obayya, M. A. Arasi, N. Alruwais, R. Alsini, A. Mohamed, and I. Yaseen, "Biomedical image analysis for colon and lung cancer detection using tuna swarm algorithm with deep learning model," *IEEE Access*, vol. 11, pp. 94705–94712, 2023, doi: 10.1109/ACCESS.2023.3309711.

## BIOGRAPHIES OF AUTHORS

**Mr. Thiyagarajan Manoharan** working as Assistant Professor in the Department of Computer Science and Engineering at VelTech Rangarajan Dr. Sagunthala R&D Institute of Science and Technology, Chennai. He has completed M.Tech Degree in Computer Science and Engineering and B.E Degree in Computer Science and Engineering. His research area of interest includes machine learning, AIoT, cyber security, cloud computing. He has totally 15 years of teaching and research experiences in various engineering colleges and universities. He has reviewed many papers in various international journals. He has published papers in national journals. He can be contacted at email: thiyaga1647@gmail.com.

**Ramalingam Velvizhi** is Assistant Professor, Department of CSE, Bharath Institute of Higher Education & Research, Tamil Nadu. She can be contacted at email: velvizhisp@gmail.com.

**Tarun Kumar Juluru** is head of the Department at SR Engineering College, Anantasagar, Hasanparthy, Telangana 506371, India. He can be contacted at email: tarunjuluru@gmail.com.

**Shoaib Kamal** working as an Associate Professor in the Department of Artificial Intelligence and Data Science, Global Academy of Technology, has above 10 years of teaching experience. He received his B.E degree in Electronics and Communication Engineering from P.A. College of Engineering, Mangalore affiliated to VTU Belagavi, M.Tech degree in Digital Electronics and Communication Engineering from Dayananda Sagar Institutions, Bangalore affiliated to VTU Belagavi and Ph.D. degree from Jodhpur National University, Jodhpur. He has published 13 research papers in refereed international journals and 09 research papers in the proceedings of various international conferences. His areas of research include AI & ML, Image Processing, and Communication systems. He is a life member of ISTE. He can be contacted at email: shoaibkamal87@gmail.com.

**Shrabani Mallick** Working at Dr. B R Ambedlar Institute of Technology as a Senior Lecturer, she passionate about academic and pedagogical innovations with the right mix of personalized education blended with technology. She can be contacted at email: shrabani.reek@gmail.com.

**Dr. Ezudheen Puliyanjalil** is working as an assistant professor at the Government Engineering College Thrissur. He completed his Ph.D. from the Indian Institute of Science Bangalore in the area of Software Verification in the year 2022. He completed his M-Tech with a gold medal from the National Institute of Technology Calicut in the year 2009. He is currently engaged in collaborative research with Prof. Rahul Gopinath of The University Sydney, Prof. Pavithra Prabhakar of Kansas State University and Prof. Deepak D'souza of Indian Institute of Science. His current research interest are automated reasoning, formal verification and small language models. He can be contacted at email: ezudheenpuliyanjalil@gmail.com.